

A COMPACT OMNIDIRECTIONAL DUAL-POLARIZED ANTENNA FOR 2.4-GHz WLAN APPLICATIONS WITH HIGHLY ISOLATED ORTHOGONAL SLOTS

Ying Liu^{*}, Jinyang Xue, Yu Cao, and Shuxi Gong

National Laboratory of Science and Technology on Antennas and Microwaves, Xidian University, Xi'an, Shanxi 710071, China

Abstract—An omnidirectional dual-polarized slot antenna with high port isolation for 2.4-GHz wireless local area network (WLAN) applications is proposed in this paper. The omnidirectional radiation patterns of the vertical polarization (VP) and horizontal polarization (HP) are achieved by individually cutting two orthogonal slots onto the metal walls of a cuboid antenna. The overall volume of the compact antenna is only $60 \times 10 \times 10 \text{ mm}^3$ ($0.488\lambda_0 \times 0.081\lambda_0 \times 0.081\lambda_0$). A prototype of the designed antenna is manufactured and tested. Both simulated and measured results show that the -10 dB impedance bandwidths of dual polarizations cover the desired band of 2.4–2.484 GHz and the port isolation, in the operating frequency, is less than -35 dB . Stable measured gains are greater than 2.75 and 1.35 dBi for the VP and HP, respectively.

1. INTRODUCTION

Nowadays polarization diversity that combines two antennas with orthogonal polarization has been widely adopted in modern wireless communication systems [1–5]. Especially in the multiple-input-multiple-output (MIMO) systems, for saving the space, dual-polarized antennas are usually used to substitute two space-isolated single-polarized antennas [6]. Such polarized MIMO antennas have been proved to show the advantages of increasing spectrum efficiency, mitigating polarization mismatch between the transmitter and the receiver, improving the channel capacity and diversity gain [7–9]. However, for the volume-limited portable devices, the mutual coupling between different polarizations must be controlled to assure the benefit of MIMO applications.

Received 24 July 2013, Accepted 22 August 2013, Scheduled 4 September 2013

* Corresponding author: Ying Liu (liuying@mail.xidian.edu.cn).

Several studies on investigating the dual-polarized antennas with different radiating structures, such as patch antennas and slot antennas, can be found in the literatures [10–13]. Among them, the radiation patterns are unidirectional [10, 11] or bidirectional [12, 13]. However, in some special conditions, it is requisite for the antennas to have omnidirectional radiation patterns to cover a large service area, such as the portable access points or base stations.

Over the last decades, a number of omnidirectional antennas with VP or HP have been developed [14–20]. In order to obtain the VP, a printed planar microstrip antenna is investigated in [14], and a similar design adopting the dipole is also reported in [15]. For the horizontally polarized omnidirectional radiation pattern, the magnetic dipole is an alternative solution. This can be achieved by a small loop with a uniform current distribution. Nevertheless, the impedance match is very difficult for the small loop due to its small dimensions. Adopting the left-hand loading loop [16] and the Alford loop structure [17] can obtain good impedance match, but which have a disadvantage of complicated configuration. Combining the vertically and the horizontally polarized antenna elements is an immediate solution to obtain dual polarizations. In [18], a notched disk antenna and a wire antenna are combined for dual polarizations, but the isolation between the two ports is only 14 dB. A dual-polarized omnidirectional planar slot antenna for 5.2-GHz WLAN applications is reported in [19]. Nevertheless, the omnidirectional planes for VP and HP are different. In [20], the dual-polarized antenna is comprised of a dielectric-loaded slotted-cylinder antenna for the HP and a conventional collinear array antenna for the VP. However, the beam gets tilted in the elevation plane thanks to the asymmetrical structure. Besides, the overall volume of the proposed antenna is also quite large for the small-volume portable devices.

This paper proposed an omnidirectional dual-polarized slot antenna with high isolation for 2.4-GHz WLAN applications. Two orthogonal slots are cut onto the four metal walls of a cuboid antenna to obtain the dual-polarized omnidirectional radiation patterns. Among them, a folded horizontal slot with two ends short-circuit is adopted for the VP. With regard to the HP, a modified vertical arc slot with two ends open-circuit is used, which has the advantages of broadening the bandwidth and increasing the magnitude of the horizontal current. The proposed antenna successfully solves two major problems of dual-polarized antenna design in a volume-limited MIMO system. One is to obtain omnidirectional radiation patterns for both VP and HP in a small volume, and the other is to decrease the mutual coupling between dual polarizations in such a compact volume. Its radiation

mechanism and equivalent structure are described in Section 2.2. Low mutual coupling between VP and HP is achieved in a very compact volume of $60 \times 10 \times 10 \text{ mm}^3$. A prototype of the proposed antenna is fabricated and tested to validate the design strategy. In Section 3, the measured results including S -parameters, radiation patterns and gains are also presented and discussed. The presented antenna displays the advantages of omnidirectional radiation, small volume and high port isolation, which shows the potential application in volume-limited WLAN MIMO antenna systems, such as portable access points and mobile terminals.

2. ANTENNA STRUCTURE AND DESIGN

2.1. Antenna Structure

The geometry of the proposed antenna is shown in Figure 1. As shown a 3-D stereogram in Figure 1(a), the antenna is mainly composed with four rectangular metal walls, which are supported by a FR4 substrate ($\epsilon_r = 4.6$, $\tan \delta = 0.015$), with a thickness of 1 mm. Two

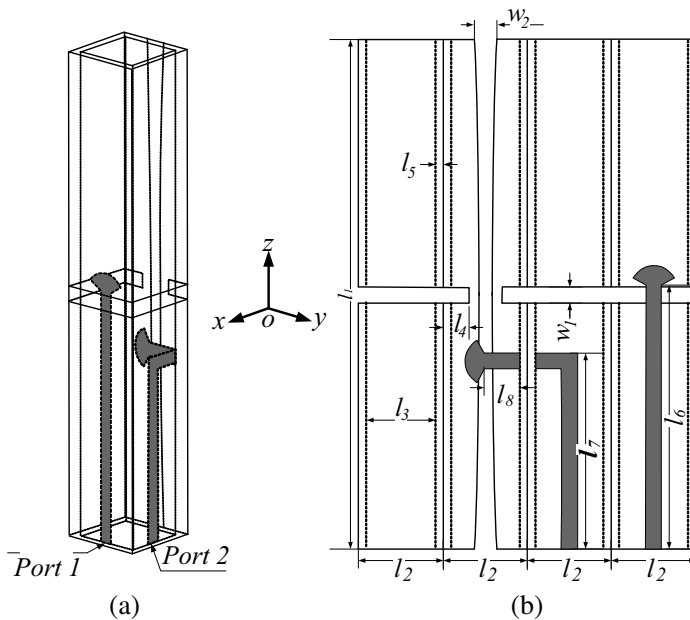


Figure 1. Geometry of the proposed antenna, (a) 3-D stereogram view, (b) expanded view.

orthogonal slots are cut from the metal walls of the cuboid antenna for the dual-polarized radiation patterns. The expanded view of the designed antenna is illustrated in Figure 1(b). The dark area expresses the feed-lines and the light area the metal walls. A vertical arc slot is cut in the center of the second metal wall, with the size $l_1 \times w_2$. A $50\text{-}\Omega$ open-ended microstrip line is used to feed the vertical slot by capacitive coupling. A horizontal slot is cut in the middle of the cuboid metal walls, with the dimension $(3 \times l_2 + 2 \times l_4) \times w_1$. It is also fed by another $50\text{-}\Omega$ open-ended microstrip line. In addition, the microstrip lines are terminated with “fan” open stubs, which can enforce the radio frequency (RF) signal to flow into the feeding slots [21]. When fed through port 1, the designed antenna operates at a VP mode. The HP mode is achieved by feeding the proposed antenna through port 2. The two orthogonal slots can provide omnidirectional patterns in the azimuthal plane with low mutual coupling and sufficient impedance bandwidth. The overall volume of the presented antenna is only $l_1 \times l_2 \times l_2 = 60 \times 10 \times 10 \text{ mm}^3$.

The simulations are implemented by applying the commercial software Ansoft High Frequency Structure Simulator (HFSS), whose algorithm is based on the finite element method. The detailed dimensions are listed in Table 1.

Table 1. Detailed dimensions of the proposed antenna (unit: mm).

<i>Parameter</i>	l_1	l_2	l_3	l_4	l_5
<i>Value</i>	60	10	8	3	1
<i>Parameter</i>	l_6	l_7	l_8	w_1	w_2
<i>Value</i>	32	23	4	1.8	2.5

2.2. Radiation Mechanism

The radiation mechanisms of the two slots are totally different. The horizontal slot is cut onto all metal walls to provide vertically polarized omnidirectional radiation pattern. Figure 2 shows the electric field magnitude distribution of the VP mode. As shown in Figure 2, the horizontal slot can be equivalent as a magnetic dipole and it works in the half-wavelength mode. Figure 3 displays the vector current distribution in the VP mode. Unlike the electric dipole, the current distribution of the magnetic dipole is not restricted in a narrow region. From Figure 3, within a certain distance, the current is guided around the edge of the horizontal slot. According to Babinet’s principle, compared with the corresponding electric dipole, the magnetic dipole



Figure 2. Electric field magnitude distribution of the VP mode fed by port 1 at 2.44 GHz.

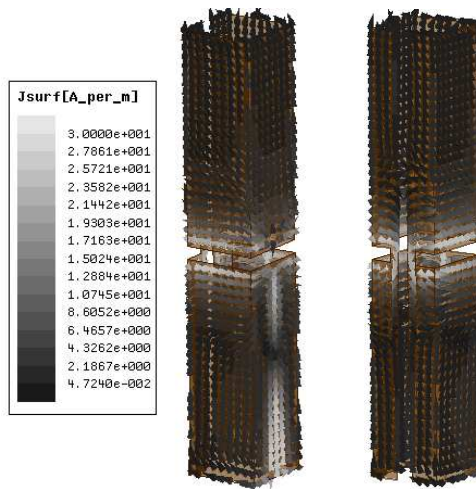


Figure 3. Vector current distribution of the VP mode fed by port 1 at 2.44 GHz.

has the same frequency characteristics. Consequently, through widening the horizontal slot can broaden the bandwidth and decrease the resonance frequency. Eventually by means of broadening the slot and with the effect of the FR4 substrate, the designed length of the

horizontal folded slot is only $3 \times l_2 + 2 \times l_4 = 36$ mm, which is much less than half-wavelength of the resonant frequency ($\lambda_0/2 = 61.48$ mm at 2.44 GHz). In addition, the horizontal slot can provide an impedance bandwidth from 2.22 to 2.68 GHz, which completely covers the desired band of 2.4–2.484 GHz.

For the HP, the vertical arc slot cut onto the second wall also provides an omnidirectional pattern with a small value of $l_1 \times w_2$. The magnitude distributions of electric field and current are shown in Figures 4 and 5, respectively. From the figures, especially intuitional in Figure 5, the radiation structure of the proposed antenna can be equivalent to a series of shunt open loop antennas. Figure 6 gives the equivalent structure of the proposed antenna. The total HP radiation pattern can be regarded as a superimposition of the loop antenna patterns. Consequently, the radiation mechanism of the presented antenna is similar to that of a conventional loop antenna. However, the vertical slot is very difficult to match in such a compact structure. The reason can be attributed to the four folded metal walls. These walls can be considered as an open-end back cavity of the vertical slot with high Q factor. In which, Q factor is inversely proportional to the antenna resonance bandwidth (Δf). When resonant at $\omega = \omega_0 = 2\pi f_0$, the Q factor of the proposed antenna can be expressed as:

$$\frac{\Delta f}{f_0} = \frac{1}{Q} \quad (1)$$

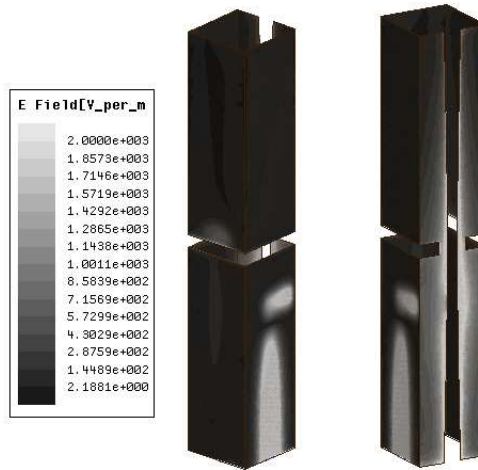


Figure 4. Electric field magnitude distribution of the HP mode fed by port 2 at 2.44 GHz.

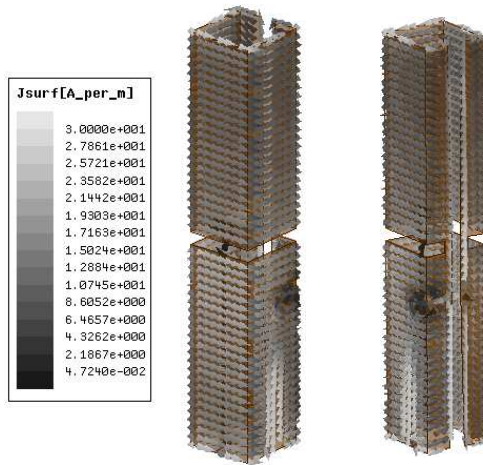


Figure 5. Vector current distribution of the HP mode fed by port 2 at 2.44 GHz.

Both the slot shape and feed will have significant impacts on the bandwidth. The Q factor can also be computed in the following equation:

$$Q = \omega_0 C_{\text{loop}} R = \frac{R}{\omega_0 L_{\text{loop}}} \quad (2)$$

where C_{loop} and L_{loop} are the equivalent capacitance and inductance of the open loop antenna, respectively. From Equations (1) and (2), it can be seen that the capacitance C_{loop} is inversely proportional to the bandwidth and the inductance L_{loop} is proportional to the bandwidth. Therefore, the bandwidth can be increased by applying a larger L_{loop} and a lower C_{loop} .

Typical shunt loop antennas can provide an ideal omnidirectional pattern, while a series of shunt open loop antennas, as indicated in Figure 6, will lead to a non-uniform radiation in the azimuthal plan due to the “field leakage” from the slots of the loop antennas. The field leakage radiation can be reduced by decreasing the width of the vertical slot. Nevertheless, it will leads to the increase of the C_{loop} , and further increase the Q factor. As a result, it will result in the decrease of the resonance bandwidth. Therefore there is a conflict between the omnidirectional radiation pattern and the resonance bandwidth. In the process of the antenna design, a compromise has been made between the bandwidth and the omnidirectional radiation pattern. Finally, the vertical slot has been matched with a -10 dB resonance bandwidth from 2.39 to 2.49 GHz.

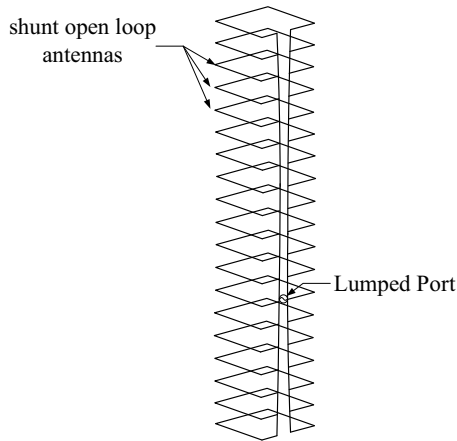


Figure 6. Equivalent shunt open loop structures of the proposed antenna.

2.3. Isolation Analysis

The mutual coupling between the two radiating elements is an important issue in the MIMO antenna design. It is a great challenge to enhance high isolation between the two ports with so compact volume. To achieve a high isolation, the two radiation slots are positioned orthogonally and symmetrically. The vector current distributions for both polarizations at central frequency are respectively investigated in Figure 3 and Figure 5 to explain the isolation enhancement method.

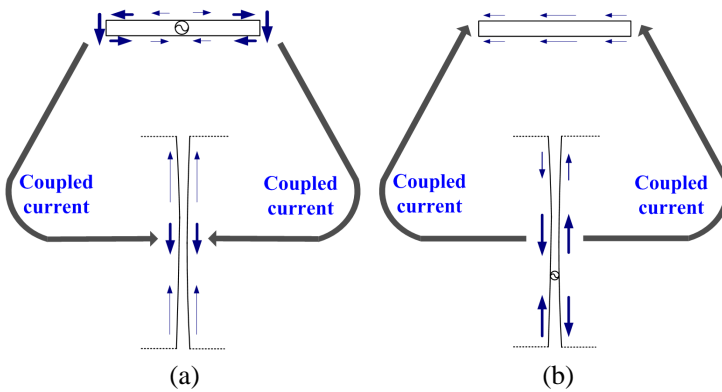


Figure 7. Current relations of two slots when the antenna fed by (a) port 1 and (b) port 2 at 2.44 GHz.

The current relations of the two radiation slots are illustrated in Figure 7. When the antenna is fed by port 1, the current on the horizontal slot is shown in Figure 7(a). Strong current on the narrow edges of the horizontal slot is coupled to the middle of the wide arc edges of the vertical slot. Nevertheless, the couple current is with the same amplitude and in phase. As a result, barely field is coupled to the vertical slot.

When the antenna is fed by port 2, the current distributions of the two slots are indicated in Figure 7(b). The coupled current on the horizontal slot is also with the almost same amplitude and in phase along two opposite wide edges. Therefore, the coupled field in the horizontal slot is extremely weak. High port isolation can be achieved by positioning two orthogonal slots.

3. EXPERIMENTAL VERIFICATION

To validate the design strategy above, a prototype of the proposed antenna is manufactured and tested. The photograph of the proposed antenna is shown in Figure 8. A series of characteristic are investigated both in simulation and measurement. The results are given as follows.

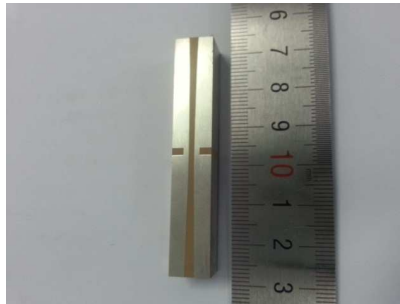


Figure 8. Photograph of the proposed antenna.

3.1. *S*-parameters

The simulated and measured *S*-parameters of the presented antenna are shown in Figure 9. As shown in Figure 9, the measured results are agreed with the simulated ones. The measured -10 dB impedance bandwidth are 2.4–2.49 GHz for the HP mode and 2.21–2.58 GHz for the VP mode, both of which cover the 2.4-GHz WLAN band of 2.4–2.484 GHz. Both the simulated and the measured isolations between the two feeding ports, in the operating frequency, are lower than -35 dB. Furthermore, it is emphasized that high port isolation is

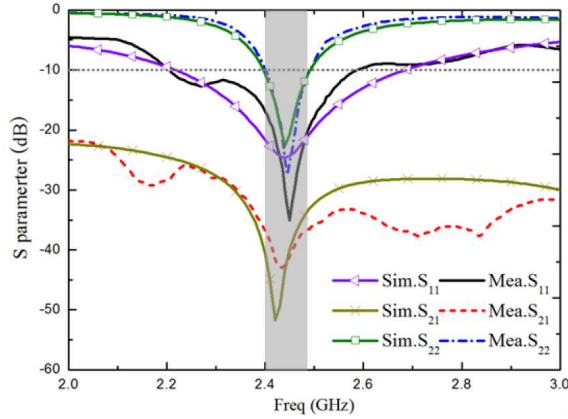


Figure 9. Simulated and measured S -parameters of the proposed antenna.

achieved in such a compact volume of $60 \times 10 \times 10 \text{ mm}^3$ ($0.488\lambda_0 \times 0.081\lambda_0 \times 0.081\lambda_0$).

3.2. Radiation Pattern

The simulated and measured radiation patterns of the proposed antenna fed by port 1 and port 2 in the xy - and xz -planes at 2.44-GHz are depicted in the Figures 10 and 11. Obviously, an omnidirectional radiation pattern is achieved in the xy -plane for both VP and HP. In addition, the measured patterns are basically consistent with the simulated ones. The differences are mainly caused by the accidental errors arising from accuracy in fabrication and the testing environment, but which are acceptable substantially. The maximum and minimum gains are 2.78 and 0.5 dBi for the VP and 1.87 and 0.9 dBi for the HP. As illustrated in Figures 10 and 11, relatively low cross-polarization level is also achieved for both polarizations.

Figure 12(a) gives the electric field magnitude distribution of the xy -plane at 2.44 GHz. When fed through port 1, as previously mentioned, the radiation mechanism of the proposed antenna can be equivalent to a folded magnetic dipole. Due to its half-wave model, the electric field magnitude distribution on the two ends of the dipole tends to be zero. As a result, there is a relatively weak radiation along $-x$ axis direction. For the HP mode, the radiation mechanism of the proposed antenna can be equivalent to a series of shunt open loop antennas. As shown in Figure 12(b), due to field leakage radiation of the vertical slot, the maximum radiation direction is along the $-x$ axis. These analyses also have been confirmed in Figures 10 and 11.

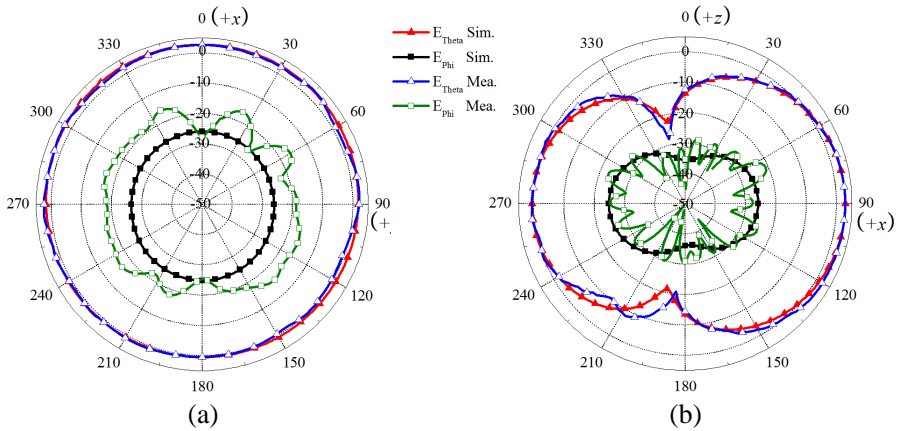


Figure 10. Simulated and measured radiation patterns of the proposed antenna fed by port 1 at 2.44 GHz in (a) xy -plane and (b) xz -plane.

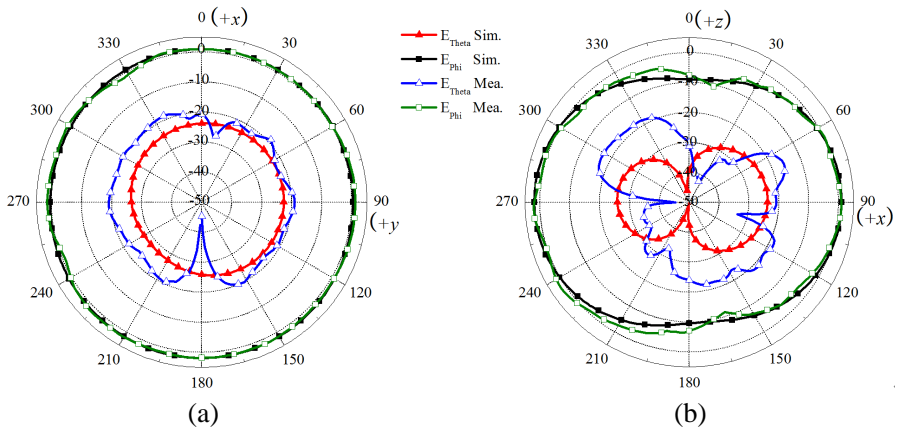


Figure 11. Simulated and measured radiation patterns of the proposed antenna fed by port 2 at 2.44 GHz in (a) xy -plane (b) xz -plane.

3.3. Gain and Radiation Efficiency

Figure 13 shows the comparison of the simulated and measured gains in the operating frequencies. Compared with the simulation results, there are some gain losses, especially when fed by port 2. The measured average gains of the proposed antenna are 2.77 and 1.72 dBi for the VP and HP, respectively. An average gain difference of 1.05 dB exists

between the two polarization modes, which is mainly because that the radiation efficiency of the vertical slot is lower than that of the horizontal slot. Figure 14 gives the simulated directivity and radiation efficiency of both polarizations. From Figure 14, the radiation efficient of the VP and the HP are 92% and 79.2%, respectively. As previously discussed, the radiation mechanisms of the two slots are different. Compared with the horizontal slot, the vertical slot has a back cavity with high Q factor. Therefore, the radiation efficiency is lower than that of a conventional slot.

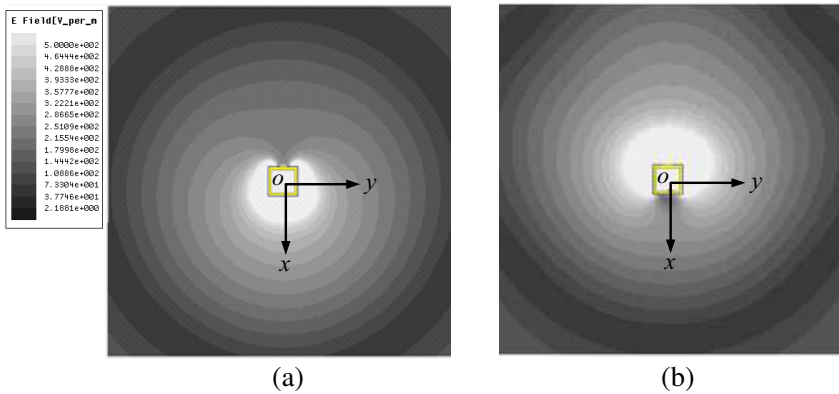


Figure 12. Electric field magnitude distribution of the xy -plane fed by (a) port 1 and (b) port 2 at 2.44 GHz.

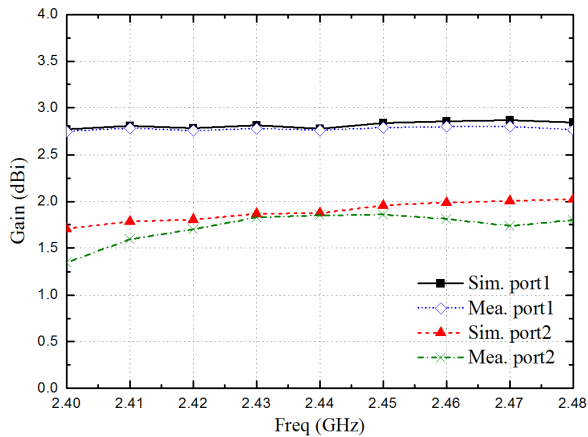


Figure 13. Simulated and measured gains of the proposed antenna.

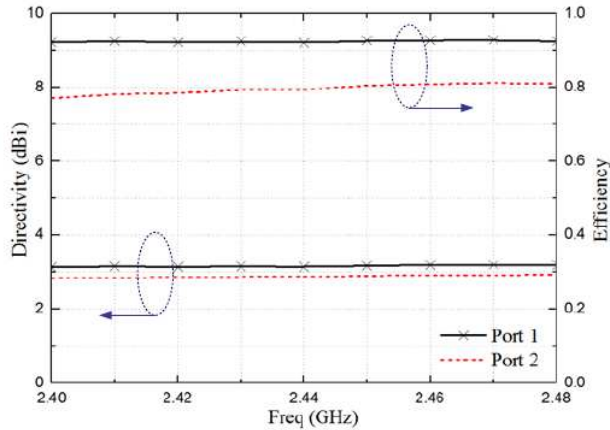


Figure 14. Simulated directivity and efficiency of the proposed antenna.

4. CONCLUSION

This paper proposes a compact dual-polarized MIMO antenna for WLAN 2.4-GHz with omnidirectional radiation pattern in the azimuthal plane. Two orthogonal slots are cut onto metal walls to provide the VP and HP. To validate the design strategy, a prototype antenna is manufactured and tested. Simulated and measured results shows that the -10 dB impedance bandwidths of the dual polarization cover WLAN 2.4–2.484 GHz. The isolation between the dual operating modes, in the operating band, is lower than -35 dB. The measured gains of the VP and HP are greater than 2.75 and 1.35 dBi, respectively. The designed antenna solves two main problems of small-volume MIMO system: achieving omnidirectional radiation patterns and reducing the mutual coupling for dual polarizations in a very compact volume. In short, the proposed antenna reveals a sufficient impedance bandwidth, high input port isolation, stable gain and omnidirectional radiation patterns. Furthermore, the overall volume of the presented antenna is only $60 \times 10 \times 10 \text{ mm}^3$ ($0.488\lambda_0 \times 0.081\lambda_0 \times 0.081\lambda_0$).

ACKNOWLEDGMENT

This work is supported by Program for New Century Excellent Talents in University (NCET-11-0690) and the Fundamental Research Funds for the Central Universities (K5051202049).

REFERENCES

1. Vongsack, S., C. Phongcharoenpanich, S. Kosulvit, K. Hamamoto, and T. Wakabayashi, "Unidirectional antenna using two-probe excited circular ring above square reflector for polarization diversity with high isolation," *Progress In Electromagnetics Research*, Vol. 133, 159–176, 2013.
2. Tu, T.-C., C.-M. Li, and C.-C. Chiu, "The performance of polarization diversity schemes in outdoor micro cells," *Progress In Electromagnetics Research*, Vol. 55, 175–188, 2005.
3. Xu, H.-X., G.-M. Wang, and M.-Q. Qi, "A miniaturized triple-band metamaterial antenna with radiation pattern selectivity and polarization diversity," *Progress In Electromagnetics Research*, Vol. 137, 275–292, 2013.
4. Chung, J.-Y., "Ultra-wideband dielectric-loaded horn antenna with dual-linear polarization capability," *Progress In Electromagnetics Research*, Vol. 102, 397–411, 2010.
5. Cao, W.-Q., B. Zhang, A. Liu, T. Yu, D. Guo, and Y. Wei, "Novel phase-shifting characteristic of CRLH TL and its application in the design of dual-band dual-mode dual-polarization antenna," *Progress In Electromagnetics Research*, Vol. 131, 375–390, 2012.
6. Jeon, K., B. Hui, K. Chang, H. Park, and Y. Park, "SISO polarized flat fading channel modeling for dual-polarized antenna systems," *IEEE 2012 International Conference on Information Networking (ICOIN)*, 368–373, 2012.
7. Molina-Garcia-Pardo, J.-M., J.-V. Rodriguez, and L. Juan-Llacer, "Polarized indoor MIMO channel measurements at 2.45 GHz," *IEEE Transactions on Antennas and Propagation*, Vol. 56, No. 12, 3818–3828, 2008.
8. Valenzuela-Valdés, J. F., et al., "Evaluation of true polarization diversity for MIMO systems," *IEEE Transactions on Antennas and Propagation*, Vol. 57, No. 9, 2746–2755, 2009.
9. Konanur, A. S., et al., "Increasing wireless channel capacity through MIMO systems employing co-located antennas," *IEEE Transactions on Microwave Theory and Techniques*, Vol. 53, No. 6, 1837–1844, 2005.
10. Wong, H., K.-L. Lau, and K.-M. Luk, "Design of dual-polarized L-probe patch antenna arrays with high isolation," *IEEE Transactions on Antennas and Propagation*, Vol. 52, No. 1, 45–52, 2004.
11. Guo, Y.-X., K.-W. Khoo, and L. C. Ong, "Wideband dual-polarized patch antenna with broadband baluns," *IEEE*

- Transactions on Antennas and Propagation*, Vol. 55, No. 1, 78–83, 2007.
12. Li, Y., et al., “A dual-polarization slot antenna using a compact CPW feeding structure,” *IEEE Antennas and Wireless Propagation Letters*, Vol. 9, 191–194, 2010
 13. Soliman, E. A., M. S. Ibrahim, and A. K. Abdelmageed, “Dual-polarized omnidirectional planar slot antenna for WLAN applications,” *IEEE Transactions on Antennas and Propagation*, Vol. 53, No. 9, 3093–3097, 2005.
 14. Bancroft, R. and B. Bateman, “An omnidirectional planar microstrip antenna,” *IEEE Transactions on Antennas and Propagation*, Vol. 52, No. 11, 3151–3154, 2004.
 15. Wong, K.-L., F.-R. Hsiao, and T.-W. Chiou, “Omnidirectional planar dipole array antenna,” *IEEE Transactions on Antennas and Propagation*, Vol. 52, No. 2, 624–628, 2004.
 16. Borja, A. L., et al., “Omnidirectional loop antenna with left-handed loading,” *IEEE Antennas and Wireless Propagation Letters*, Vol. 6, 495–498, 2007.
 17. Ahn, C.-H., S.-W. Oh, and K. Chang, “A dual-frequency omnidirectional antenna for polarization diversity of MIMO and wireless communication applications,” *IEEE Antennas and Wireless Propagation Letters*, Vol. 8, 966–969, 2009.
 18. Kuga, N., H. Arai, and N. Goto, “A notch-wire composite antenna for polarization diversity reception,” *IEEE Transactions on Antennas and Propagation*, Vol. 46, No. 6, 902–906, 1998.
 19. Soliman, E. A., M. S. Ibrahim, and A. K. Abdelmageed, “Dual-polarized omnidirectional planar slot antenna for WLAN applications,” *IEEE Transactions on Antennas and Propagation*, Vol. 53, No. 9, 3093–3097, 2005.
 20. Ando, A., A. Kondo, and S. Kubota, “A study of radio zone length of dual-polarized omnidirectional antennas mounted on rooftop for personal handy-phone system,” *IEEE Transactions on Vehicular Technology*, Vol. 57, No. 1, 2–10, 2008.
 21. Manna, A., P. Baldonero, and F. Trotta, “Novel UWB low-profile sinuous slot antenna,” *IEEE Proceedings of the 5th European Conference on Antennas and Propagation (EUCAP)*, 783–786, 2011.